

Eur. Phys. J. A (2018) 54: 225

DOI 10.1140/epja/i2018-12659-2

Measurement of the analyzing powers in $\vec{p}d$ elastic and $\vec{p}n$ quasi-elastic scattering at small angles

S. Barsov et al.



Measurement of the analyzing powers in $\vec{p}d$ elastic and $\vec{p}n$ quasi-elastic scattering at small angles

S. Barsov^{1,a}, Z. Bagdasarian^{2,3}, S. Dymov^{4,5}, R. Gebel³, M. Hartmann³, A. Kacharava³, I. Keshelashvili³, A. Khokkaz⁶, V. Komarov⁴, P. Kulesa⁷, A. Kulikov⁴, A. Lehrach³, N. Lomidze², B. Lorentz³, G. Macharashvili², D. Mchedlishvili^{2,8}, S. Merzliakov^{4,3}, S. Mikirtychyants¹, M. Nioradze², D. Prasuhn³, F. Rathmann³, D. Schröder⁶, V. Serdyuk³, V. Shmakova⁴, R. Stassen³, H. Ströher³, M. Tabidze², A. Täschner⁶, S. Trusov^{9,10}, D. Tsirkov⁴, Yu. Uzikov^{4,10,11}, Yu. Valdau^{1,3}, and C. Wilkin^{12,b}

¹ St. Petersburg Nuclear Physics Institute, NRC Kurchatov Institute, RU-188350 Gatchina, Russia

² High Energy Physics Institute, Tbilisi State University, GE-0186 Tbilisi, Georgia

³ Institut für Kernphysik, Forschungszentrum Jülich, D-52425 Jülich, Germany

⁴ Laboratory of Nuclear Problems, JINR, RU-141980 Dubna, Russia

⁵ University of Ferrara and INFN, I-44100 Ferrara, Italy

⁶ Institut für Kernphysik, Universität Münster, D-48149 Münster, Germany

⁷ H. Niewodniczański Institute of Nuclear Physics PAN, PL-31342 Kraków, Poland

⁸ SMART|EDM-Lab, Tbilisi State University, GE-0179 Tbilisi, Georgia

⁹ Institut für Kern- und Hadronenphysik, Forschungszentrum Rossendorf, D-01314 Dresden, Germany

¹⁰ Department of Physics, M. V. Lomonosov Moscow State University, RU-119991 Moscow, Russia

¹¹ Dubna State University, RU-141980 Dubna, Russia

¹² Physics and Astronomy Department, UCL, London WC1E 6BT, UK

Received: 6 August 2018 / Revised: 8 November 2018

Published online: 19 December 2018

© The Author(s) 2018. This article is published with open access at Springerlink.com

Communicated by N. Kalantar

Abstract. The analyzing powers in proton-deuteron elastic and proton-neutron quasi-elastic scattering have been measured at small angles using a polarized proton beam at the COSY storage ring incident on an unpolarized deuterium target. The data were taken at 796 MeV and five higher energies from 1600 MeV to 2400 MeV. The analyzing power in pd elastic scattering was studied by detecting the low energy recoil deuteron in telescopes placed symmetrically in the COSY plane to the left and right of the beam whereas for pn quasi-elastic scattering a low energy proton was registered in one of the telescopes in coincidence with a fast scattered proton measured in the ANKE magnetic spectrometer. Though the experiment explores new domains, the results are consistent with the limited published information.

1 Introduction

The nucleon-nucleon (NN) interaction is of great importance in any study of hadronic processes at intermediate energies. At such energies a full set of amplitudes may be extracted using a phase-shift analysis but this is obviously dependent on the availability of a reliable experimental data base. Proton-proton elastic scattering has been extensively studied in many laboratories worldwide, including at the COoler SYnchrotron (COSY) of the Forschungszentrum Jülich [1–8]. The wealth of spin-dependent quantities measured has allowed the extraction of NN phase shifts in the isospin $I = 1$ channel up to al-

most 3000 MeV [9, 10]. The situation is far less promising for the isoscalar channel where the much poorer neutron-proton data base only permits the $I = 0$ phase shifts to be evaluated up to at most 1300 MeV, but with significant ambiguities above about 800 MeV.

Small angle neutron-proton elastic scattering has been studied at COSY over recent years by measuring the interaction of a deuteron beam with a hydrogen target [11, 12]. However, in this case the maximum beam energy at COSY is about 1150 MeV/nucleon. To go higher in energy, where np data are very scarce, measurements have to be performed using a proton beam incident on a deuterium target.

The differential cross section [8] and analyzing power [7] in proton-proton elastic scattering have been studied at COSY using the ANKE magnetic spectrometer. Despite

^a e-mail: barsov_sg@pnpi.nrcki.ru

^b e-mail: c.wilkin@ucl.ac.uk (corresponding author)

the ANKE acceptance and experimental capabilities for investigating pn elastic scattering becoming much less favourable as the beam energy increases, it was considered a priority for the ANKE Collaboration to contribute to the pn elastic data base above 1500 MeV by measuring the proton analyzing power.

The elements of ANKE that were used in this experiment are described in sect. 2. These are the forward detector, in which fast protons were measured, and the silicon tracking telescopes (STT) that were used to measure low energy protons and deuterons. Since the results were obtained with a polarized proton beam, its preparation and measurement were integral to the success of the proposal. However, the experiment was carried out just after the measurement of the analyzing power in proton-proton elastic scattering [7] using the same beam so that the presentation in sect. 3 can be relatively brief.

Proton-deuteron elastic scattering could be cleanly identified and measured by detecting the deuteron in one of the STT without the use of the forward detector. As described in sect. 4, with two STT placed symmetrically (left and right) around the target to form a two-arm polarimeter, the proton analyzing power in pd elastic scattering could be measured in a way that is completely analogous to the analyzing power measurement in pp elastic scattering [7]. There are published measurements of the proton analyzing power in proton-deuteron elastic scattering at 800 MeV over a wide angular range [13] but the later data at 796 MeV [14] cover our angular range more comprehensively and the experimental techniques employed are very similar to ours. Though our measurements at 796 MeV are consistent with these results to within experimental uncertainties [14], there are no other data at 1600 MeV and above with which to make comparisons.

The measurement of the analyzing power in proton-neutron quasi-elastic scattering, which is the subject of sect. 5, is much more challenging. There are several measurements of the analyzing power in neutron-proton elastic scattering in the 800 MeV region by different groups [15–20] some using beams of free neutrons while others studied quasifree scattering. A useful summary of the available data is to be found on the SAID WEB site [9]. There are far fewer data available at our higher energies and those that exist tend to cover only the larger angles. The two exceptions are the measurements carried out at 2205 MeV [21,22]. Though the $pd \rightarrow ppn$ reaction can be selected by measuring one fast proton in the forward detector and a slow proton in an STT, there is then the difficulty of identifying quasi-free elastic pn collisions and avoiding regions where the NN final state interaction (FSI) is very strong. Ideally, the contamination from these effects would be studied with the help of a full reaction model but, in its absence, one has to resort to a more empirical approach.

The pn FSI, which can lead in particular to the refraction of a deuteron, decreases fast with the momentum transfer, as does the pd elastic differential cross section itself. Furthermore, the contribution from quasi-free scattering on the neutron in the deuteron is enhanced in regions where the “spectator” proton momentum is small

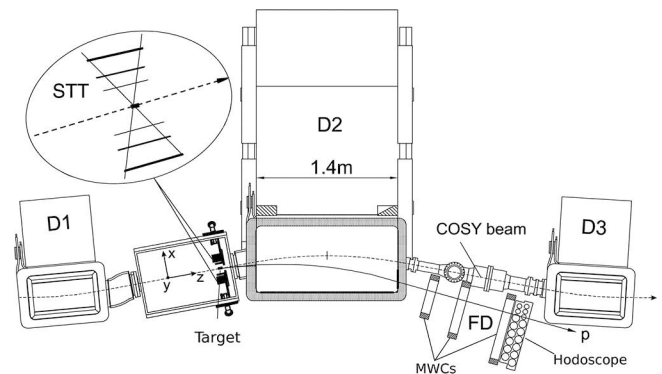


Fig. 1. The ANKE spectrometer setup (top view), showing the positions of the deuterium cluster-jet target, the silicon tracking telescopes (STT), and the forward detector (FD).

compared to the overall momentum transfer (q). Both these features can be exploited by making appropriate kinematic cuts. This empirical approach was tested successfully on data taken at 796 MeV.

Unlike proton-deuteron elastic scattering, the left-right symmetry is lost when measuring analyzing powers with a combination of an STT and the forward detector. One is then left with a one-arm polarimeter that relies on measurements of the intensities of the polarized beams as well as their polarizations. Nevertheless, the results obtained are consistent with the limited available published information. Our conclusions are drawn in sect. 6.

2 Experimental setup

The experiment was carried out using the ANKE magnetic spectrometer [23] positioned inside the COSY storage ring [24] of the Forschungszentrum Jülich. Although the facility sketched in fig. 1 was equipped with other elements, the only detectors used in this experiment were the forward detector (FD) and the silicon tracking telescopes (STT) [25].

Fast protons arising from small-angle proton-deuteron elastic scattering or quasi-free elastic scattering on the constituent nucleons were measured in the FD in the range 4° – 10° in laboratory polar angle (θ_{lab}) and 160° – 200° in azimuthal angle (ϕ). The forward detector comprises a set of multiwire proportional and drift chambers and a two-plane scintillation hodoscope. In addition to their use for triggering, the scintillators were also needed to measure the energy losses required for particle identification [26].

The two STT were installed in the COSY plane symmetrically inside the vacuum chamber to the left and right of the beam at distances of 3 cm from the deuterium cluster-jet target, which had a jet diameter of about 1 cm [27]. Each telescope consists of three position-sensitive silicon layers of $70 \mu\text{m}$, $300 \mu\text{m}$, and 5 mm thickness and, in this configuration, covered laboratory polar angles $75^\circ < \theta_{\text{lab}} < 140^\circ$. The acceptances of the STT in azimuth of $\pm 30^\circ$ were centred at $\phi = 0^\circ$ and $\phi = 180^\circ$ on the left and the right sides, respectively.

Protons and deuterons were clearly identified by the $dE-E$ technique when they passed through the first layer and were stopped in the second or third layer of an STT. These conditions are realized for protons with kinetic energies between 2.5 and 30 MeV and for deuterons between 3.5 and 40 MeV. The momenta of these low energy protons and deuterons were determined using the position information from the first and the second layers and their total energy loss. The relative positions of the silicon detectors in the first and the second layers were directly measured in the laboratory with a precision of ± 0.1 mm. The front-end electronics of the STT provided the self-triggering signal from the second layers (*STT-trigger*).

3 Polarized proton beam

The ANKE experiment used a vertically polarized beam incident on an unpolarised target and the preparation of the beam and the measurement of its polarization were carried out in common with the studies of the analyzing powers in proton-proton elastic scattering [7]. H^- ions, with either spin up (\uparrow) or down (\downarrow), were supplied by the polarized ion source. These were then accelerated to 45 MeV in the cyclotron JULIC before being stripped of their electrons and injected into the COSY ring [28]. The sign of the polarization was flipped at every beam injection at the beginning of the acceleration cycle. The polarization of the injected beam was optimized using a low energy polarimeter in the injection beam line to COSY [29]. In both spin modes, source polarizations of about 0.93 were achieved and the difference between their values was measured to be smaller than the statistical uncertainty of 1%.

In a strong-focusing synchrotron, such as COSY, resonances can lead to losses of polarization of a proton beam during acceleration. In order to compensate for these effects, adiabatic spin-flip was used to overcome the imperfection resonances and tune-jumping to deal with the intrinsic ones [30]. The beam polarization after acceleration was measured using the EDDA detector as a polarimeter. This detector, originally equipped with a polarized hydrogen target, had been used to measure the analyzing power in elastic proton-proton scattering at larger angles over almost the whole COSY energy range [3,4]. By studying further the scattering of polarized protons on C and CH_2 targets, it was possible to deduce the quasi-free analyzing power of carbon, where the necessary calibration standard was provided by the EDDA $p\bar{p}$ data [31].

The simplified version of the EDDA detector that was used in the present experiment was equipped with a $7\ \mu\text{m}$ diameter carbon fibre target that could be moved in and out of the beam. The polarimeter, which had been calibrated during the EDDA data-taking periods against the full detector setup, consists of 29 pairs of half-rings placed to the left and right of the beam. The left-right asymmetry of counts is determined for each pair of half-rings, thus providing a dependence on the polar angle θ_{lab} while averaging over the azimuthal angle ϕ in every half-ring. The systematic uncertainty of the measurements was estimated to be 3% [31].

Table 1. The mean values of beam polarizations P determined with the EDDA polarimeter averaged over all the data at the beam energy T_p in MeV. The changes in the sign of P are due to the spin flips induced when passing through the imperfection resonances. Though the statistical errors shown are small, there are 3% systematic uncertainties [31].

| T_p | 796 | 1600 | 1800 | 1965 | 2157 | 2368 |
|-------|-------------|-------------|-------------|-------------|-------------|-------------|
| P | 0.511 | 0.388 | -0.476 | -0.508 | -0.513 | 0.501 |
| | ± 0.001 | ± 0.003 | ± 0.007 | ± 0.009 | ± 0.011 | ± 0.007 |

The experiment was carried out at six proton kinetic energies, $T_p = 796, 1600, 1800, 1965, 2157,$ and 2368 MeV. Cycles of 180 s or 300 s duration were used, with the last 20 s of each cycle being reserved for the measurement of the beam polarization with the EDDA polarimeter [32]. Mean values of the beam polarizations determined from the EDDA data at the six energies are given in table 1. It should be noted that the values correspond to half the difference between spin-up and spin-down data because the simplified variant of the EDDA detector does not allow the determination of the polarization for each spin mode individually. The changes in sign reflect the number of spin flips required to pass through the imperfection resonances. Since each of the six beams was prepared independently by the COSY crew, the magnitude of the polarization need not decrease monotonically as further resonances are crossed.

4 Analyzing power in proton-deuteron elastic scattering

Elastic proton-deuteron scattering was the only source of low energy deuterons that fell within the angular acceptance of the STT. This reaction can therefore be reliably identified by just evaluating the information provided by STT. For this purpose, events were recorded using the *STT-trigger*, which requested a minimal energy deposit in the second layer of either of the two STT telescopes. The deuterons were then easily selected from energy loss measurements in the silicon layers. As a consequence, it is not surprising that the missing-mass distributions in the $pd \rightarrow dX$ reaction measured in either STT showed only clear peaks, well centred at the proton mass, with very little background, as illustrated in fig. 2 using data from one STT at a beam energy of 796 MeV. The positions of these peaks were independent of the deuteron kinetic energy (T_d). In both STT the peaks had the same widths of $15.6\ \text{MeV}/c^2$ ($FWHM$), as averaged over the total T_d range. The widths increased significantly with decreasing T_d , due to small angle scattering of the deuterons in the first and second layers of the STT.

From the numbers of deuterons detected in the left (L_d) and right (R_d) telescopes during each acceleration cycle, the asymmetry of $\bar{p}d$ elastic scattering was evaluated for each pair of successive cycles with beam polarizations up and down, using the cross-ratio method [33],

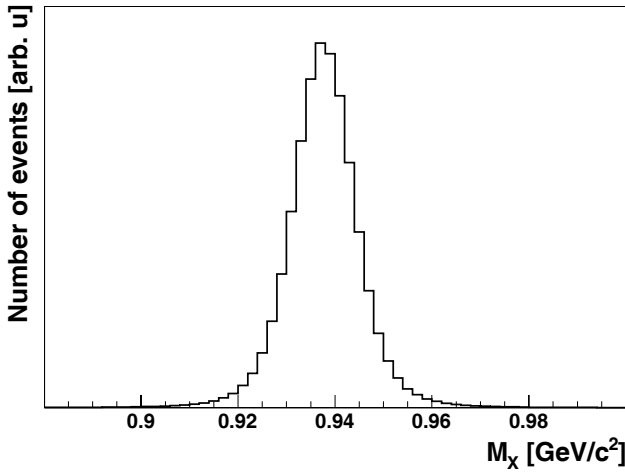


Fig. 2. The missing-mass distribution for the $pd \rightarrow dX$ reaction at $T_p = 796$ MeV where the slow deuteron was detected in the left-side STT. Since no information from the forward detector was used here, the widths of the distributions are almost independent of beam energy. For the same reason, the results obtained from the two STT yield, of course, indistinguishable missing-mass distributions.

which eliminates first-order systematic errors. It was carefully studied in ref. [32] for the $\bar{p}p$ elastic data, which were taken under similar conditions but with the hydrogen cluster target. None of the cycles were used twice and for each beam energy the asymmetry over the data-taking period was quite stable and the result constant to within statistical uncertainties. These data thus allowed us to detect if there were any variation of the beam polarization cycle by cycle. The L_d/R_d ratio, which was calculated for each cycle, was constant within statistical errors for each of the two spin modes. This indicates that, not only the beam polarization, but also the acceptances of the STT, were quite stable during measurements at all beam energies. Less than 1% of cycles at each beam energy were found to show any significant deviation of the L_d/R_d ratio from its average value. The data from these cycles were not considered in the subsequent analysis.

The angular dependence of the proton analyzing power in $\bar{p}d$ elastic scattering was determined from the *STT-trigger* data for all six beam energies and the results are shown in fig. 3 in terms of the c.m. momentum transfer q . The numerical values at all six energies are presented in table 2 as a function of the scattering angle Θ_{cm} . The values of Θ_{cm} and q were determined from the deuteron kinetic energy, which was measured in the STT to much higher accuracy than the polar angle. The deuteron energy was measured with about a 2% uncertainty, which would correspond to an uncertainty in Θ_{cm} of less than 0.2° in the angular range below 20° , which is small compared to the 1° bins that we have used for the data.

Data were also taken with a trigger that combined signals from the FD and STT. The combined results with the *STT-* and *FdSTT-triggers* were largely consistent with those using the *STT-trigger* with an RMS deviation over all energies of about 2%. Combining this with the 3% un-

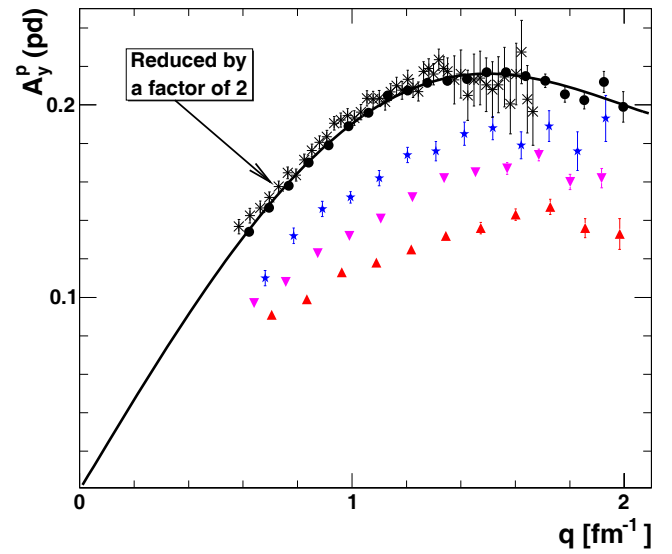


Fig. 3. The proton analyzing power $A_y^p(pd)$ in proton-deuteron elastic scattering as a function of the momentum transfer q in the centre-of-mass frame. ANKE data at 796 MeV are shown by closed (black) circles, at 1600 MeV by (blue) stars, at 1965 MeV by (magenta) inverted triangles, and at 2368 MeV by (red) triangles. Only statistical errors are shown and in general these are smaller than the symbol size. The fit of eq. (1) to the ANKE data at 796 MeV is shown by the continuous curve. The LAMPF data at this energy are shown by (black) crosses [14]. In order to increase the visibility of the higher energy points, the ANKE and LAMPF results and the curve at 796 MeV are reduced by a factor of two. The numerical values of the ANKE data are to be found in table 2.

certainty in the beam polarizations leads to a total systematic uncertainty of 4%.

On general grounds the proton analyzing power¹ is of the form of q times a function of q^2 and the ANKE 796 MeV results of fig. 3 are well described by

$$A_y^p(pd) = 0.4714q - 0.0987q^3 + 0.0077q^5. \quad (1)$$

This form also reproduces very well the LAMPF data [14] provided that it is multiplied by a factor of 1.021. This 2% difference is to be compared with the 3% precision in the beam polarization measurements with EDDA [31], which is our dominant systematic uncertainty, and the 2% systematic uncertainty in the LAMPF beam polarization [34,35]. An uncertainty of 2% in the deuteron kinetic energy E_d corresponds to 1% in the momentum transfer $q \approx \sqrt{2m_d E_d}$ and, using eq. (1), less than 1% in the analyzing power. This uncertainty is similar at the higher energies.

The only obvious theoretical description of proton-deuteron elastic scattering data is the refined Glauber model of Platonova and Kukulín [36]. As in the original

¹ We use a notation where $A_y^p(pd)$ is the proton analyzing power in pd elastic scattering and $A_y^p(pn)$ is the same in pn elastic scattering. The deuteron vector analyzing power in dp elastic scattering is denoted by $A_y^d(dp)$.

Table 2. Analyzing power $A_y^p(pd)$ in $\bar{p}d$ elastic scattering at six proton kinetic energies marked in the separate columns in MeV in angular bins of 1° . The systematic errors, which are not shown, are dominated by the 4% combined uncertainty in the beam polarization and the trigger selection.

| Θ_{cm} degrees | $A_y^p(pd : 796)$ | $A_y^p(pd : 1600)$ | $A_y^p(pd : 1800)$ | $A_y^p(pd : 1965)$ | $A_y^p(pd : 2157)$ | $A_y^p(pd : 2368)$ |
|--------------------------|-------------------|--------------------|--------------------|--------------------|--------------------|--------------------|
| 5.5 | – | – | 0.128 ± 0.004 | 0.097 ± 0.002 | 0.092 ± 0.003 | 0.091 ± 0.002 |
| 6.5 | – | 0.110 ± 0.004 | 0.138 ± 0.002 | 0.108 ± 0.002 | 0.105 ± 0.002 | 0.099 ± 0.002 |
| 7.5 | – | 0.132 ± 0.004 | 0.149 ± 0.002 | 0.123 ± 0.002 | 0.113 ± 0.002 | 0.113 ± 0.002 |
| 8.5 | 0.268 ± 0.004 | 0.146 ± 0.004 | 0.162 ± 0.002 | 0.132 ± 0.001 | 0.126 ± 0.002 | 0.118 ± 0.002 |
| 9.5 | 0.293 ± 0.003 | 0.152 ± 0.003 | 0.171 ± 0.002 | 0.141 ± 0.002 | 0.133 ± 0.002 | 0.125 ± 0.002 |
| 10.5 | 0.316 ± 0.003 | 0.162 ± 0.004 | 0.188 ± 0.002 | 0.152 ± 0.002 | 0.142 ± 0.003 | 0.132 ± 0.002 |
| 11.5 | 0.340 ± 0.003 | 0.174 ± 0.004 | 0.193 ± 0.003 | 0.162 ± 0.002 | 0.149 ± 0.003 | 0.136 ± 0.003 |
| 12.5 | 0.358 ± 0.003 | 0.176 ± 0.005 | 0.198 ± 0.003 | 0.165 ± 0.002 | 0.155 ± 0.003 | 0.143 ± 0.003 |
| 13.5 | 0.378 ± 0.002 | 0.185 ± 0.006 | 0.207 ± 0.003 | 0.167 ± 0.003 | 0.161 ± 0.004 | 0.147 ± 0.004 |
| 14.5 | 0.392 ± 0.003 | 0.188 ± 0.006 | 0.214 ± 0.004 | 0.174 ± 0.003 | 0.160 ± 0.005 | 0.136 ± 0.005 |
| 15.5 | 0.410 ± 0.003 | 0.179 ± 0.007 | 0.208 ± 0.005 | 0.160 ± 0.004 | 0.153 ± 0.006 | 0.133 ± 0.008 |
| 16.5 | 0.415 ± 0.003 | 0.189 ± 0.008 | 0.204 ± 0.006 | 0.162 ± 0.005 | 0.150 ± 0.011 | – |
| 17.5 | 0.423 ± 0.003 | 0.176 ± 0.010 | 0.205 ± 0.008 | – | – | – |
| 18.5 | 0.425 ± 0.004 | 0.193 ± 0.012 | – | – | – | – |
| 19.5 | 0.427 ± 0.004 | – | – | – | – | – |
| 20.5 | 0.434 ± 0.004 | – | – | – | – | – |
| 21.5 | 0.434 ± 0.005 | – | – | – | – | – |
| 22.5 | 0.430 ± 0.005 | – | – | – | – | – |
| 23.5 | 0.425 ± 0.007 | – | – | – | – | – |
| 24.5 | 0.411 ± 0.008 | – | – | – | – | – |
| 25.5 | 0.405 ± 0.009 | – | – | – | – | – |
| 26.5 | 0.424 ± 0.011 | – | – | – | – | – |
| 27.5 | 0.398 ± 0.016 | – | – | – | – | – |

Glauber spinless work [37], there are contributions from single and double scattering that involve, respectively, the interaction with one or two nucleons in the deuteron. However, the nucleon-nucleon amplitudes used as input in the refined model retain all the five spin-dependent pp and pn terms so that predictions can be made of the polarization observables in pd elastic scattering. Using the updated SAID NN partial wave analysis [38], Platonova and Kukulkin predicted the angular dependence of $A_y^p(pd)$ at 800 MeV in the refined Glauber model [39]. Though the structure that they found is similar to that of the experimental data, their calculations underestimate the experimental data at low q shown in fig. 3. No reliable predictions could be made at our higher energies due to the lack of a pn partial wave analysis above 1.3 GeV.

By using only the information provided by the STT, there was a symmetric setup that is certainly preferable for the measurements of an analyzing power. However, the left-right symmetry is broken when information from the forward detector is required, as it is in the measurement of quasi-elastic scattering, to which we now turn.

5 Analyzing power in quasi-elastic proton-neutron scattering

Events corresponding to the breakup reaction $pd \rightarrow ppn$ can be identified by measuring a fast proton in the forward detector and a slow one in one of the STT. These then provide a missing-mass distribution for the $pp \rightarrow ppX$ reaction and this is illustrated in fig. 4 for a beam energy of 1800 MeV. The neutron peak is well separated from the inelastic continuum and the background under the peak is only a few percent. Apart from the ambiguities of the background, the $pd \rightarrow ppn$ events are fully reconstructed so that it is possible to study regions of quasi-elastic pn scattering.

Having identified the $pd \rightarrow ppn$ events, the next task is to isolate quasi-free elastic $pn \rightarrow pn$ and, in particular, to remove contamination from quasi-elastic scattering on the proton in the deuteron. This was first studied in simulations of the $pd \rightarrow ppn_{\text{spec}}$ and the $pd \rightarrow pnp_{\text{spec}}$ reactions within the framework of a simple incoherent “spectator” model, which has been used successfully in the mea-

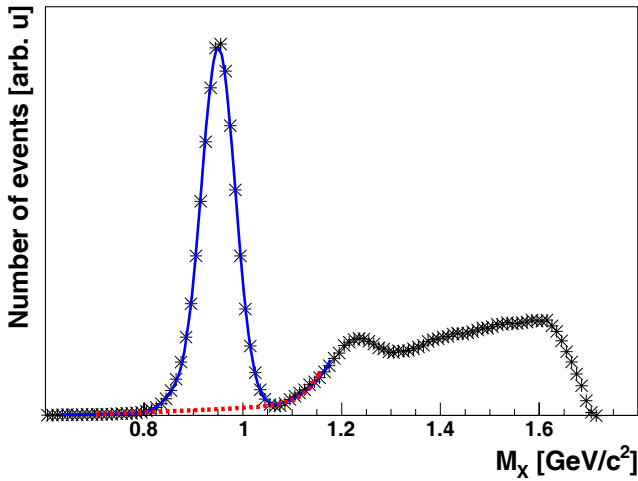


Fig. 4. Missing-mass M_X spectra obtained for the $pd \rightarrow ppX$ reaction at a beam energy of 1800 MeV when detecting one proton in the right side STT and the other one in the FD. This distribution shows a clear neutron peak with little background, estimated by the (red) dashed line of linear plus exponential terms fitted using data from outside the peak region. It is possible that the start of the continuum reveals evidence for $\Delta(1232)$ excitation. The solid (blue) curve represents the Gaussian + background fit to data in the neutron peak region.

surement of spin observables with a polarized deuteron beam [17]. The Fermi motion of nucleons in the deuteron was taken into account using the Paris model [40] but, in the absence of information at the higher energies, the differential cross sections for free pn elastic scattering was assumed to be equal to that of pp except in the Coulomb interaction region. The events generated were convoluted with the ANKE acceptance using the GEANT program package [41].

As illustrated in fig. 5, even at the lowest beam energy, the count rate from the $pd \rightarrow ppn_{\text{spec}}$ reaction was found in the simulation to be strongly suppressed kinematically compared with $pd \rightarrow pnp_{\text{spec}}$ when the slow proton was detected in the right-side STT [42]. This is due to the asymmetric acceptance of the FD and, for this reason, only data from the right-side STT were analyzed in terms of quasi-elastic scattering on the neutron. This configuration also reduces the contribution from the FSI between the “spectator” proton and the recoil neutron. Despite the very simplified model used in the simulations, the momentum and angular distributions for low energy protons in events that formed the peak in fig. 4 were found to be very similar to the simulated distributions for “spectator” protons emitted from the $pd \rightarrow pnp_{\text{spec}}$ reaction. The count rate from quasi-free pp is expected in this model to be less than 5% of that from quasi-free pn even at the 796 MeV. At higher beam energies the limit reduces to below 3%.

Under the experimental conditions described above, the ANKE system operated as a single-arm polarimeter, which means that the analyzing power had to be deduced from the asymmetry of counts corresponding to different

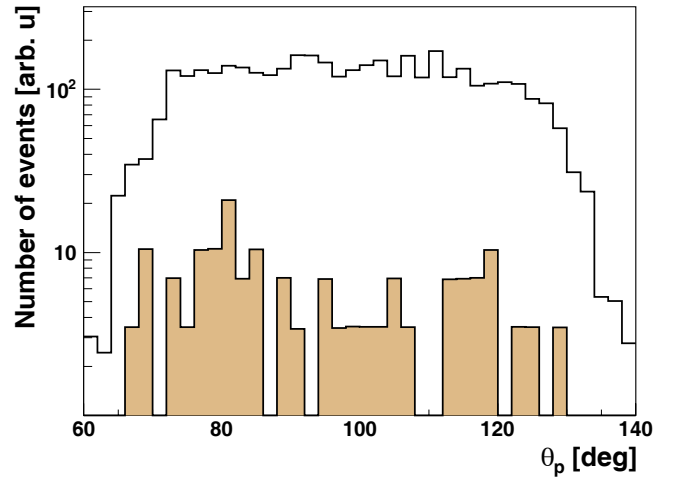


Fig. 5. Count rates for the $pd \rightarrow ppn_{\text{spec}}$ (brown shading) and $pd \rightarrow pnp_{\text{spec}}$ (black lines) reactions simulated within the framework of the incoherent “spectator” model at $T_p = 800$ MeV. A fast proton is detected in the FD and a slow one in the right-side STT at a laboratory angle θ_p .

orientations of the beam polarization. Such an asymmetry is very sensitive to the relative luminosities of the beams with spin up and down. The ratio of luminosities for P^\uparrow and P^\downarrow , integrated over a certain period of data taking, was determined from the numbers of deuterons detected in both STT during the same period, as described for elastic $\bar{p}d$ scattering in sect. 4. If $|P^\uparrow| = |P^\downarrow|$ and the STT acceptances were stable, the combination $(L_d^\uparrow \cdot R_d^\uparrow)/(L_d^\downarrow \cdot R_d^\downarrow)$ would be equal to the ratio of the squares of the luminosities, convoluted with the “dead-time” of readout system [33]. However, these limitations should not be significant in our case. For example, because the $\bar{p}d$ asymmetry is less than 0.2 in our experiment, a 20% difference between $|P^\uparrow|$ and $|P^\downarrow|$ would induce a systematic effect in $A_y^p(pn)$ that is below 1%. A large difference in the STT acceptances for different spin modes would also manifest itself in measurements of $A_y^p(pd)$ presented in the previous section. Any significant effect can be excluded here by comparing the 796 MeV ANKE and LAMPF data [14] shown in fig. 3.

The ratio of luminosities obtained in this way could be unambiguously applied for the normalization of the quasi-elastic data if these had been obtained using the *STT-trigger*. However, most of the *STT-trigger* rate was produced by particles that were accompanied by protons that did not fall within the FD acceptance. In the more selective *FdSTT-trigger*, a coincidence was also demanded between a *STT-trigger* signal and a signal in the forward detector. Furthermore, in order to increase the number of events recorded with the *FdSTT-trigger*, the *STT-trigger* rate was significantly pre-scaled. Despite the whole ANKE detection system being read out for any trigger, the “dead-time” corrections for data sets taken with different triggers might still differ, and this has to be taken into account. Nevertheless, it was found in a special investigation that the ratio of the average “dead-time” factors obtained from

data with beam polarization up and down were nearly equal for both the *STT-trigger* and the *FdSTT-trigger* data. The maximum deviation between the two results was about 1% but, on average, it was closer to 0.5%.

The use of the ratio of luminosities derived from the numbers of deuterons detected in both STT was also verified through the analysis of proton-deuteron elastic events selected from data measured with both triggers. Such a comparison was feasible because the *STT-trigger* rate was significantly pre-scaled so that it contained only a few percent of events recorded with the *FdSTT-trigger*. As stressed in the previous section, the values of $A_y^p(pd)$ obtained using the cross-ratio method are insensitive to the integrated luminosities convoluted with the corresponding “dead-time” factors. In the case of the *FdSTT-trigger*, the $\bar{p}d$ elastic events were selected by requiring the coincidence of a proton detected in the FD with a deuteron identified in the left side STT. The momentum of the fast proton was reconstructed in the same way as for pn quasi-elastic events.

The angular dependence of the pd elastic asymmetry derived from data measured at 796 MeV with the *FdSTT-trigger* is perfectly consistent with that obtained in ref. [14] and shown in fig. 3. Furthermore, the average beam polarization of 0.502 ± 0.002 , determined by scaling our measured asymmetries to their analyzing powers, differs from the value obtained with the EDDA polarimeter by only 2%. At higher beam energies, where no other measurements of the analyzing power have been found, the asymmetry obtained from the *FdSTT-trigger* data was compared with that deduced from the *STT-trigger* data using the cross-ratio method. The results were found to be in good agreement in angular regions where there was an overlap. A systematic difference of about 4% was observed at 2157 MeV, though differences below 2% were found at all the other energies. These differences can be taken as estimates of the overall systematic uncertainties when determining asymmetries with a single-arm polarimeter. In addition to possible changes in acceptance for different spin modes, there are also systematic uncertainties arising from possible differences between beam polarizations $|P^\uparrow|$ and $|P^\downarrow|$ after acceleration.

As shown in fig. 4, the background under the neutron peak at 1800 MeV was only about 6%, and this was similar at other beam energies. If the background analyzing power is large, it could nevertheless affect the results because the $\bar{p}n$ asymmetry is typically about 0.1 or even less. The background contribution was therefore evaluated for each angular bin and the asymmetry corrected. When applying this correction, it was important to ensure that the background was independent of beam polarization. For this purpose, missing-mass distributions measured with P^\uparrow and P^\downarrow for each energy were normalized to have equal luminosity and then subtracted. For all the energies above 796 MeV the resulting distributions contained only the neutron peak, which was very well fit by a Gaussian distribution with no background. However, due to a small number of deuterons originating from the $\bar{p}d \rightarrow p_{\text{spec}}d\pi^0$ reaction, the background in the vicinity of the peak at the

lowest beam energy was found to depend on the polarization. After eliminating these events by using the energy-loss information from the FD scintillation hodoscope, the residual background was also shown to be polarization independent. The systematic uncertainty arising from the description of the background under the peak was estimated to be about 1.5%.

Taking into account the 3% systematic error in the measurements of the beam polarization with EDDA, we estimate that the overall systematic uncertainty in the measurement of the analyzing power in $\bar{p}n$ elastic scattering is about 5.5% at 2157 MeV but below 4% at the other beam energies. These systematic effects are smaller than the typical statistical errors of about 10%.

In earlier experiments [15,21,22], quasi-free $A_y^p(pn)$ was studied by measuring both scattered particles in conditions close to free kinematics and then reconstructing the momentum of the unobserved “spectator” proton. In contrast, at ANKE the fast scattered proton was detected in coincidence with the directly measured “spectator” proton. The quasi-free scenario is generally assumed to be realized when the momentum transfer from a beam particle to a scattered one (p_T) is large compared with the “spectator” particle momentum (p_{spec}), which should correspond to the Fermi momentum in the deuteron. It is clearly desirable to determine experimentally the values of p_{spec}/p_T for which the “spectator” model is valid. This will be influenced by the design of the STT, which requires a proton to have a momentum above 70 MeV/c in order to be reconstructed.

The applicability of the “spectator” model was tested in the 796 MeV data. Although only the laboratory momentum transfer range $100 < p_T < 260$ MeV/c was here accessed, this was the only energy where several experiments on quasi-free $\bar{p}p$ and $\bar{p}n$ elastic scattering were performed [15,43,19,20] and which were used in the derivation of the stable solution (SP07) of the SAID phase-shift analysis [9,10].

It is interesting to note that the $\bar{p}n$ analyzing power obtained without any restriction on the p_{spec}/p_T ratio was found to be in good agreement with the SP07 prediction over the whole of the ANKE angular acceptance which, at this beam energy, is $10^\circ < \Theta_{cm} < 25^\circ$. However, it is difficult to believe that the “spectator” model could be still valid when $p_{\text{spec}}/p_T > 0.5$ as this corresponds to $\Theta_{cm} < 15^\circ$, *i.e.*, a region where the pn final state interaction is very strong. The dependence of the analyzing power on the p_{spec}/p_T ratio was therefore investigated separately in different Θ_{cm} ranges.

The results for $20^\circ < \Theta_{cm} < 24^\circ$, which correspond to momentum transfers $200 < p_T < 260$ MeV/c, are presented in the lower panel of fig. 6. The minimum value of p_{spec}/p_T allowed by the ANKE setup at this energy is 0.3 but the values obtained for $A_y^p(pn)$ remain close to the SP07 prediction up to $p_{\text{spec}}/p_T \simeq 0.6$. Using the conservative upper limit of $p_{\text{spec}}/p_T < 0.5$, values of the analyzing power were obtained that were in good agreement with the SP07 solution as well as with the data measured in ref. [15] down to $\Theta_{cm} = 17^\circ$, as shown in the upper panel

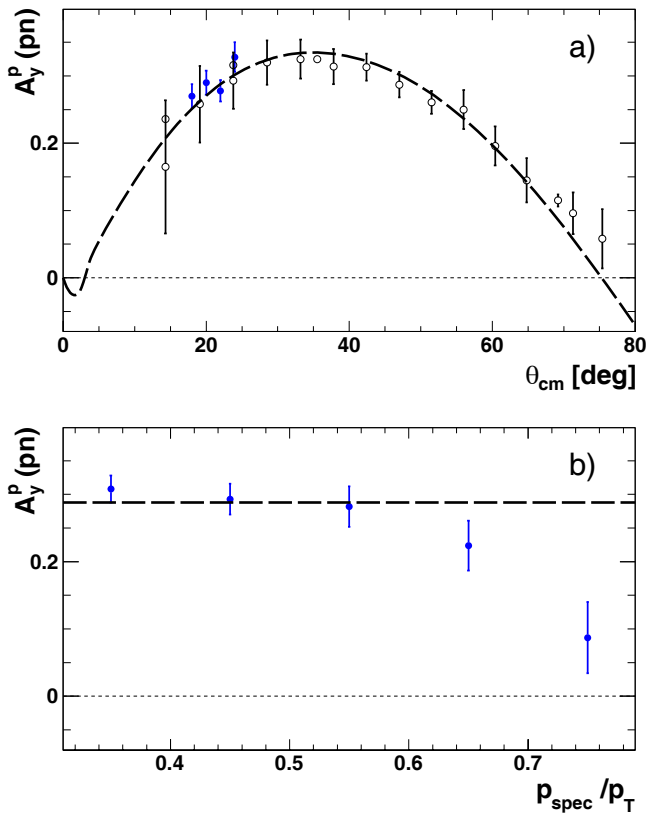


Fig. 6. Analyzing power $A_y^p(pn)$ in quasi-free $\bar{p}n$ elastic scattering at $T_p \approx 796$ MeV. Panel (a): the open points are results from ref. [15] as a function of the centre-of-mass scattering angle θ_{cm} . The blue solid points show results from the current experiment extracted, as discussed in the text, under conditions where $p_{spec}/p_T < 0.5$ and $p_T > 200$ MeV/c, where p_T is the laboratory momentum transfer. The predictions of the SAID SP07 partial wave solution [10] are shown by the dashed curve. Panel (b): the values of $A_y^p(pn)$ measured at ANKE for $\theta_{cm} = 22^\circ \pm 2^\circ$ as a function of the p_{spec}/p_T ratio. The horizontal dashed line indicates the SAID SP07 solution for $A_y^p(pn)(\theta_{cm} = 22^\circ)$ [10].

of fig. 6 (see footnote²). However, for angles smaller than 17° the dependence of $A_y^p(pn)$ on p_{spec}/p_T was less credible. The analyzing power near the lower limit of p_{spec}/p_T allowed by the FD acceptance was found to be unexpectedly larger than that predicted by the SP07 solution and it decreased monotonically with increasing p_{spec}/p_T . This means that the analyzing power measured for $\theta_{cm} < 17^\circ$ with the $p_{spec}/p_T < 0.5$ cut deviates significantly from the expected angular dependence. This deviation can be ascribed to the final state interaction between the recoiling neutron and proton, which increases in importance as p_T is reduced.

The value of $\theta_{cm} = 17^\circ$ at 796 MeV corresponds to a momentum transfer of 180 MeV/c and the data at the various energies reported in table 3 were all obtained with

² In order to improve the clarity of the figure, data from other experiments are not presented here.

the restriction $p_T > 190$ MeV/c as well as $p_{spec}/p_T < 0.5$. This value of p_T is at the lower edge of the momentum transfer range covered by the FD detector at 1600 MeV and at higher energies it is well outside the range and therefore does not introduce extra cuts.

The values of the analyzing power shown in table 3 generally decrease with increasing beam energy and the results presented in fig. 7 illustrate the scale of the dependence. Despite the different experimental approach, the ANKE results at 2200 MeV are fully consistent with data from refs. [21,22]. As was stressed already, the data base on pn elastic scattering observables is insufficient to yield reliable partial wave solutions above about 1300 MeV. It is therefore not surprising that the SAID SP07 solution [10] does not predict well our new experimental data shown in fig. 7. However, the SAID solution was recently updated [38] to take into account the experimental data measured at COSY-WASA [44]. Although it was asserted that the new AD14 solution [38] is still valid only up to 1300 MeV, it, nevertheless, gives predictions that are much closer to our 1600 MeV data shown in fig. 7 than those of SP07 [10].

6 Conclusions

We have measured the analyzing power in $\bar{p}d$ elastic and $\bar{p}n$ quasi-elastic scattering at 796 MeV and at five energies from 1600 MeV to 2400 MeV at the COSY-ANKE facility. The results at 796 MeV are consistent with published data to within the quoted uncertainties. The $\bar{p}d$ elastic measurements at 1600 MeV and above were carried out for the first time at small angles and there is little $\bar{p}n$ elastic information at these higher energies.

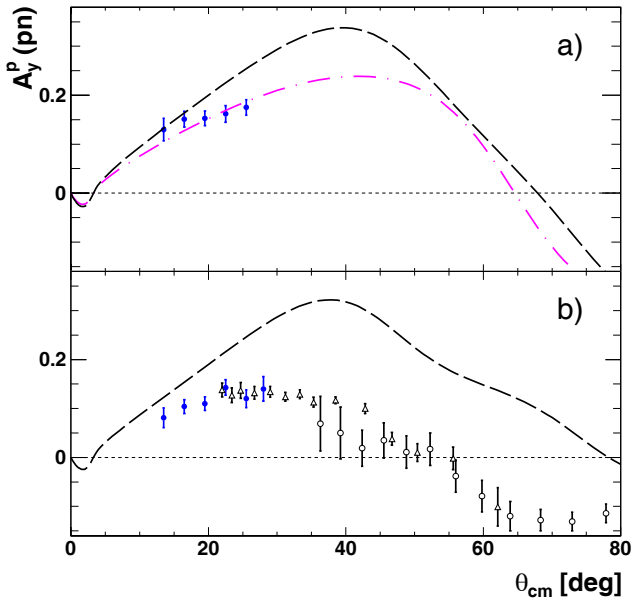
The results on $\bar{p}d$ elastic scattering were obtained using two silicon tracking telescopes as a two-arm polarimeter. In this case the systematic uncertainty was dominantly associated with the calibration of the EDDA beam polarimeter, which is known with an accuracy of about 3%. Our results at 796 MeV lie about 2% lower than the previous measurements [14] but are easily consistent within the systematic uncertainties of both experiments.

The analyzing power in $\bar{p}d$ elastic scattering at higher energies was found to be about a factor of two smaller than at the 796 MeV and generally decreasing with beam energy. The decrease of analyzing power with energy is similar to that noted for the deuteron analyzing power in $\bar{d}p$ elastic scattering [45–48]. This similarity is not surprising because it has been argued in connection with the 796 MeV data [14] that the proton analyzing power at small angles is determined mainly by the interference of the charge-average central NN amplitude with the spin-orbit term. This should also be true for the deuteron analyzing power, though there are of course different modifications of the polarizations due to the multiple scatterings.

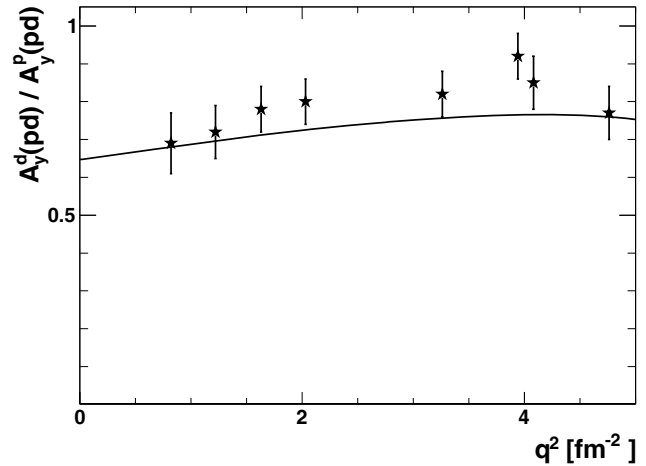
In the single scattering approximation the dominant NN amplitudes, where one neglects the spin-spin term, would suggest that the ratio $R = A_y^d(dp)/A_y^p(pd)$ should be constant with a value of 2/3. Parameterizing all the

Table 3. Analyzing power $A_y^p(pn)$ in $\vec{p}n$ quasi-elastic scattering measured at six proton kinetic energies T_p ; Only statistical errors are shown.

| T_p MeV | Θ_{cm} degrees | $A_y^p(pn)$ | T_p MeV | Θ_{cm} degrees | $A_y^p(pn)$ | T_p MeV | Θ_{cm} degrees | $A_y^p(pn)$ |
|--------------|--------------------------|-------------------|--------------|--------------------------|-------------------|--------------|--------------------------|-------------------|
| 796 | 18.0 | 0.270 ± 0.018 | 1600 | 13.5 | 0.130 ± 0.023 | 1800 | 13.5 | 0.125 ± 0.011 |
| | 20.0 | 0.290 ± 0.018 | | 16.5 | 0.151 ± 0.016 | | 16.5 | 0.147 ± 0.009 |
| | 22.0 | 0.278 ± 0.017 | | 19.5 | 0.153 ± 0.015 | | 19.5 | 0.156 ± 0.009 |
| | 24.0 | 0.328 ± 0.022 | | 22.5 | 0.162 ± 0.017 | | 22.5 | 0.149 ± 0.009 |
| | | | | 25.5 | 0.175 ± 0.016 | | 25.5 | 0.163 ± 0.010 |
| 1965 | 14.0 | 0.115 ± 0.022 | 2157 | 13.5 | 0.081 ± 0.020 | 2368 | 17.5 | 0.088 ± 0.012 |
| | 16.5 | 0.125 ± 0.013 | | 16.5 | 0.104 ± 0.014 | | 20.5 | 0.112 ± 0.013 |
| | 19.5 | 0.127 ± 0.014 | | 19.5 | 0.110 ± 0.014 | | 23.5 | 0.107 ± 0.015 |
| | 22.5 | 0.130 ± 0.015 | | 22.5 | 0.143 ± 0.016 | | 27.0 | 0.120 ± 0.016 |
| | 25.5 | 0.146 ± 0.018 | | 25.5 | 0.120 ± 0.018 | | | |
| | | | 28.0 | 0.140 ± 0.025 | | | | |

**Fig. 7.** $A_y^p(pn)$ of quasi-free $\vec{p}n$ elastic scattering at (a) 1600 MeV and (b) 2200 MeV as function of the centre-of-mass scattering angle Θ_{cm} . Solid (blue) points show the values obtained in the ANKE experiment whereas open (black) points are results taken from ref. [21] (triangles) and ref. [22] (circles). The magenta dot-dashed curve represents the new AD14 SAID solution at 1600 MeV [38], though it should be noted that this energy is outside the stated range of validity of this solution. The dashed (black) curves in both panels illustrate the previous SAID solution [10], though it must be stressed that this also has limited validity above 1300 MeV.

NN amplitudes using the SAID SP07 partial wave solution [10] and including multiple scatterings in an extended Glauber model [36] gives the curve shown in fig. 8. It is here compared to data extracted from refs. [45,46] combined with the current results. Several systematic effects in the NN input cancel in the prediction of the analyzing

**Fig. 8.** The ratio between the vector analyzing power of the deuteron to that of the proton in pd elastic scattering at 796 MeV per nucleon. The values of $A_y^d(dp)$ of ref. [45] have been read from a figure produced by the same group [46] whereas those of $A_y^p(pd)$ were taken from the fit of eq. (1) to the current data. The curve represents the results of an extended multiple scattering model using the formulae given in ref. [36]. The results are presented as a function of q^2 and the largest scattering angle shown corresponds to $\Theta_{cm} \approx 30^\circ$.

power ratio. However, one is always left with systematic uncertainties in the ratio arising from the measurements of the deuteron (4%) and proton (3%) polarizations. Nevertheless, the comparison shown in fig. 8 does suggest that the proton and deuteron analyzing powers are strongly linked.

Since it is not possible to detect neutrons at ANKE, the analyzing power in proton-neutron elastic scattering was studied in quasi-free conditions using a deuterium target. This was accomplished by measuring the fast scattered proton in the forward detector in coincidence with the low energy “spectator” proton from the $\vec{p}d \rightarrow pnp_{\text{spec}}$

reaction being measured in one of the silicon tracking telescopes. This scheme relies completely on the simple “spectator” model. The validity of the empirical “spectator” approach with our kinematic cuts was tested by comparing our result at 796 MeV with data from other experiments [15, 43, 19, 20] as well as with the SP07 SAID partial wave solution [9, 10]. It seems from this that the “spectator” model can be used if the p_{spec}/p_T ratio is restricted to be below 0.5 and $p_T > 190$ MeV/c. These criteria were then applied in the analysis of our higher energy data. Good agreement was found between our data at 2157 MeV and the results from other experiments [21, 22], despite the different experimental approaches. Systematic uncertainties of our results were estimated to be about 5.5% at this energy and about 4% at others.

Just as for proton-deuteron elastic scattering, the analyzing power in quasi-elastic $\bar{p}n$ scattering at higher energies is almost a factor of two smaller than at 796 MeV. There is also a similar general decrease with increasing beam energy. However, the analyzing power at high energy is significantly less than that found in $\bar{p}p$ elastic scattering [7].

We are grateful to other members of the ANKE Collaboration for their help with this experiment and to the COSY crew for providing such good working conditions. Useful discussions took place with M.N. Platonova and J. Haidenbauer regarding the extended Glauber calculations. This material is based upon work supported by the Forschungszentrum Jülich (COSY-FEE) and the Shota Rustaveli National Science Foundation Grant 09-1024-4-200.

Open Access This is an open access article distributed under the terms of the Creative Commons Attribution License (<http://creativecommons.org/licenses/by/4.0>), which permits unrestricted use, distribution, and reproduction in any medium, provided the original work is properly cited.

References

1. D. Albers *et al.*, Phys. Rev. Lett. **78**, 1652 (1997).
2. D. Albers *et al.*, Eur. Phys. J. A **22**, 125 (2004).
3. M. Altmeier *et al.*, Phys. Rev. Lett. **85**, 1819 (2000).
4. M. Altmeier *et al.*, Eur. Phys. J. A **23**, 351 (2005).
5. F. Bauer *et al.*, Phys. Rev. Lett. **90**, 142301 (2003).
6. F. Bauer *et al.*, Phys. Rev. C **71**, 054002 (2005).
7. Z. Bagdasarian *et al.*, Phys. Lett. B **739**, 152 (2014).
8. D. Mchedlishvili *et al.*, Phys. Lett. B **755**, 92 (2016).
9. R.A. Arndt, I.I. Strakovsky, R.L. Workman, Phys. Rev. C **62**, 034005 (2000).
10. R.A. Arndt, W.J. Briscoe, I.I. Strakovsky, R.L. Workman, Phys. Rev. C **76**, 025209 (2007) <http://gwdac.phys.gwu.edu>.
11. D. Mchedlishvili, PhD Thesis (2013) available from collaborations.fz-juelich.de/ikp/anke/internal.shtml.
12. P. Adlarson *et al.*, Phys. Rev. Lett. **112**, 202301 (2014).
13. E. Winkelmann *et al.*, Phys. Rev. C **21**, 2535 (1980).
14. F. Irom, G.J. Igo, J.B. McClelland, C.A. Whitten Jr., M. Bleszynski, Phys. Rev. C **28**, 2380 (1983).
15. M.L. Barlett *et al.*, Phys. Rev. C **27**, 682 (1983).
16. B.H. Silverman *et al.*, Nucl. Phys. A **449**, 763 (1989).
17. J. Bystričký *et al.*, Nucl. Phys. A **444**, 597 (1985).
18. M.W. McNaughton *et al.*, Phys. Rev. C **53**, 1092 (1996).
19. G. Glass *et al.*, Phys. Rev. C **41**, 2732 (1990).
20. G. Glass *et al.*, Phys. Rev. C **47**, 1369 (1993).
21. R. Diebold *et al.*, Phys. Rev. Lett. **35**, 632 (1975).
22. Y. Makdisi *et al.*, Phys. Rev. Lett. **45**, 1529 (1980).
23. S. Barsov *et al.*, Nucl. Instrum. Methods Phys. Res. A **462**, 364 (2001).
24. R. Maier *et al.*, Nucl. Instrum. Methods Phys. Res. A **390**, 1 (1997).
25. R. Schleichert *et al.*, IEEE Trans. Nucl. Sci. **50**, 301 (2003).
26. S. Dymov *et al.*, Part. Nucl. Lett. **2(119)**, 40 (2004).
27. A. Khokkaz *et al.*, Eur. Phys. J. D **5**, 275 (1999).
28. P.D. Eversheim *et al.*, AIP Conf. Proc. **293**, 92 (1993).
29. D. Chiladze *et al.*, Phys. Rev. ST Accel. Beams **9**, 050101 (2006).
30. A. Lehrach *et al.*, AIP Conf. Proc. **675**, 153 (2003).
31. E. Weise, PhD Thesis, University of Bonn (2000).
32. Z. Bagdasarian, S. Dymov, G. Macharashvili, ANKE internal reports (2014) available from collaborations.fz-juelich.de/ikp/anke/internal.shtml.
33. G.G. Ohlsen, P.W. Keaton Jr., Nucl. Instrum. Methods **109**, 41 (1973).
34. M.W. McNaughton, Los Alamos Scientific Laboratory Report No. LA-8307-MS, 1980 (unpublished).
35. M.W. McNaughton *et al.*, Phys. Rev. C **23**, 838 (1981).
36. M.N. Platonova, V.I. Kukulini, Phys. Rev. C **81**, 014004 (2010).
37. R.J. Glauber, Phys. Rev. **100**, 242 (1955).
38. R.L. Workman, W.J. Briscoe, I.I. Strakovsky, Phys. Rev. C **93**, 045201 (2016).
39. M.N. Platonova, V.I. Kukulini, in preparation.
40. M. Lacombe *et al.*, Phys. Lett. B **101**, 139 (1981).
41. S. Agostinelli *et al.*, Nucl. Instrum. Methods Phys. Res. A **506**, 250 (2003).
42. S. Barsov *et al.*, IKP Annual Report (2013) available from collaborations.fz-juelich.de/ikp/anke/internal.shtml.
43. J. Ball *et al.*, Nucl. Phys. A **559**, 489 (1993).
44. P. Adlarson *et al.*, Phys. Rev. Lett. **112**, 202301 (2014).
45. M. Haji-Saied *et al.*, Phys. Rev. C **36**, 2010 (1987).
46. V. Ghazikhanian *et al.*, Phys. Rev. C **43**, 1532 (1991).
47. J. Arvieux *et al.*, Nucl. Instrum. Methods Phys. Res. A **273**, 48 (1988).
48. D. Mchedlishvili *et al.*, Nucl. Phys. A **977**, 14 (2018).